PROGRESS
IN COLOR, COLORANTS AND COATINGS

available online @ www.pccc.icrc.ac.ir

Prog. Color Colorants Coat. 9 (2016), 117-134

Ministry of Science, Research and Technology
Institute for Color Science and Technology

Corrosion Inhibition of Mild Steel in Acidic Solution by Apricot Gum as a Green Inhibitor

A. Mohammadi [1], S. M. A. Hosseini [1], M. J. Bahrami [2] and M. Shahidi [3*]

[1] Department of Chemistry, Shahid Bahonar University of Kerman, P.O. Box: 76169-14111, Kerman, Iran.

[2] Department of Science, Farhangian University, P.O. Box: 76175173, Kerman, Iran.

[3] Department of Chemistry, Kerman Branch, Islamic Azad University, P.O. Box: 7635131167, Kerman, Iran.

ARTICLE INFO

Article history:
Received: 16 Feb 2016
Final Revised: 27 Apr 2016
Accepted: 03 May 2016
Available online: 03 May 2016

Keywords:
Apricot gum
Electrochemical impedance spectroscopy (EIS)
Electrochemical noise resistance
Phosphoric acid
Green inhibitor
Wavelet analysis

ABSTRACT

The inhibitive effect of apricot gum (AG) on mild steel in 0.5 M phosphoric acid solution was investigated by potentiodynamic polarization, electrochemical impedance spectroscopy (EIS), linear polarization resistance and electrochemical noise (EN) techniques. The inhibition efficiency increased with AG concentration up to a certain value and decreased with increasing temperature. Polarization curves indicated that AG acts as a mixed type inhibitor. The EN data were analyzed by statistical and wavelet methods. The results obtained from analysis of EN data was in good agreement with those achieved by the polarization and EIS measurements. The adsorption of the inhibitor on the alloy surface in 0.5 M H_3PO_4 followed the Langmuir isotherm. According to the calculated values of both free energy and enthalpy of adsorption, it was revealed that the adsorption of inhibitor on the steel surface was a combination of physical and chemical adsorption. The morphologies of the uninhibited and inhibited mild steel surfaces in 0.5 M H_3PO_4 which were analyzed by scanning electron microscope (SEM) showed that the alloy surface damage is significantly decreased due to the presence of inhibitor. Prog. Color Colorants Coat. 9 (2016), 117-134 © Institute for Color Science and Technology.

1. Introduction

The protection of metals against corrosion by H_3PO_4 has been the subject of much study since it has been used in many industrial processes especially in fertilizer production [1]. Mild steel has been extensively studied from both theoretical and practical viewpoints [2, 3]. Mild steel is subjected to several industrial processes such as acid pickling, acid cleaning, acid descaling and oil well acidizing. However the main problem of applying mild steel is its dissolution in acidic solutions. Several methods are available for corrosion prevention. Employing inhibitors is one of the cost effective protection methods of metals and alloys in acids. Most of the acid corrosion inhibitors are heterocyclic organic

---

*Corresponding author: shahidi@iauk.ac.ir

compounds containing N, S, O and aromatic rings [4, 5]. The problem is that most of these compounds are toxic and dangerous to humans and the environment. Thus, the development of corrosion inhibitors with natural source which are non-toxic or low-toxic has been considered to be important [6, 7]. Throughout the ages, plants have been used by human beings for their basic needs such as production of food-stuffs, shelters, clothing, fertilizers, flavors and fragrances, medicines and last but not least, as corrosion inhibitors. The use of natural products as corrosion inhibitors can be traced back to the 1930's when plant extracts of Chelidoniummajus (Celandine) and other plants were used for the first time in H_2SO_4 pickling baths [8]. The strict environmental legislations and increasing ecological awareness among scientists have led to the development of "green" alternatives to mitigate corrosion. Plant extracts are incredibly rich sources of naturally synthesized chemical compounds (e.g. amino and organic acids, glucosinolates, alkaloids, polyphenols, tannins) and most are known to have inhibitive action. The uses of the natural products as corrosion inhibitors for different metals have been reported by several authors [9-13]. Most of the natural products are nontoxic, biodegradable and readily available and renewable sources of materials. Moreover, they can be extracted by simple procedures with low cost. It is well established that corrosion inhibition occurs via adsorption of inhibitor molecules on the corroding metal surface and the efficiency of inhibition depends on the mechanical, structural and chemical characteristics of the adsorption layers formed under particular conditions.

There are some conventional electrochemical methods such as electrochemical impedance spectroscopy (EIS), polarization and electrochemical noise (EN) to monitor the corrosion of metals. EN is a promising technique for corrosion analysis which has gained popularity in the recent years [14, 15]. Electrochemical noise refers to the spontaneous fluctuations in current between two coupled working electrodes (via a zero resistance ammeter (ZRA) and also spontaneous potential fluctuations of these two electrodes with respect to a reference electrode [16]. The main approaches used to analyze the EN signals are statistical, Fourier transform (FT) and wavelet transform (WT) techniques. Wavelet transform is a data analysis procedure without the precondition of stationarity or linearity [17, 18]. Statistical analysis of EN data in the time domain also could provide several important parameters such as standard deviation and electrochemical noise resistance [19]. The inverse wavelet transform can produce partial signals of the original signal. Each partial signal is a signal which resembles the fluctuations of the original signal at a particular timescale. The standard deviation of partial signal (SDPS) can indicate the variations in the intensity of the partial signal about its mean, which could be an indication of the intensity of electrochemical activity on the surface of the electrodes within a particular interval of frequency [18]. The plot of the SDPSs versus their corresponding crystal name is called SDPS plot.

Statistical analysis of EN data in the time domain could provide several important parameters such as standard deviations of potential and current, localization index and electrochemical noise resistance (R_n). R_n is calculated as the standard deviation of potential divided by the standard deviation of current [20]:

$$R_n = \frac{\sigma_V}{\sigma_I} \qquad (1)$$

where, R_n is electrochemical noise resistance, σ_V and σ_I are the standard deviations of potential and current, respectively. Therefore, it is necessary to limit the effects of drift by suitable trend removal prior to statistical analysis [21]. It was found in a recent paper that the trend removal through wavelet analysis is the preferred technique to remove drift [22].

The aim of the present work is to investigate the inhibition action of apricot gum (AG) for the corrosion of mild steel. The inhibition effect of AG was evaluated by means of various techniques including potentiodynamic polarization, EIS, LPR, EN, scanning electron microscopy (SEM) and Fourier transform infrared spectroscopy (FT-IR).

2. Experimental

Potentiodynamic polarization, LPR, EIS and EN measurements were used to study the corrosion behavior of carbon steel in 0.5 M H_3PO_4 solution without and with addition of different concentrations of apricot gum. The specimens were connected to a copper wire at one end, and then sealed using epoxy resin with the other end exposed as the working electrode (WE) surface. Before performing experiments, the WE surface was abraded by wet abrasive papers through 400–2500 grades, washed with distilled water, degreased with acetone and finally dried in air. Potentiodynamic polarization, LPR, EIS and EN experiments were conducted using a potentiostat/galvanostat Autolab 302 N supported by a frequency response analyzer FRA-2 and Nova 1.10 software. The electrochemical sequence was EN and afterwards EIS, LPR and potentiodynamic polarization measurements, respectively. A platinum plate electrode was used as the counter electrode (CE) and a saturated calomel electrode (SCE) as reference electrode and the working electrode (WE) is made of mild steel st60. The composition (wt%) of the mild steel was: C (0.15), Si (0.72), Mn (0.73), Fe (balance).

To determine the optimal concentration of inhibitor, electrochemical experiments were performed in the concentration range of 25-100 ppm. For the polarization measurement, the potential of the electrode was scanned from -200 to +200 mV versus corrosion potential at a scan rate of 1 mV/s. Linear polarization resistance (LPR) was also performed for the specimen in different inhibitor concentrations from −20 mV to +20 mV around corrosion potential by 1 mV/s scan rate. The LPR value was derived by calculating the slope of current–potential plot at corrosion potential. The frequency range in EIS experiments was 100 mHz up to 100 kHz and the amplitude was 10 mV. Two nominally identical mild steel samples with the same area (1 cm^2) were used as working electrodes in the EN measurements. The electrochemical potential and current noise were simultaneously measured in a freely corroding system including two working electrode and a saturated Hg/Hg_2Cl_2 reference electrode. The working electrodes were facing each other vertically at a distance of about 2 cm. The EN measurements were conducted at open-circuit potential. The EN data collection was started after the WEs were immersed in solution. A period of 900 s was set for each EN recording run. Noise data were analyzed with wavelet technique using the orthogonal Daubechies wavelets of the fourth order (db4). The statistical parameters were calculated after wavelet trend removal method. The sampling frequency for the electrochemical noise data was 4 Hz.

FT-IR spectra were recorded in a BRUKER spectrophotometer, which extended from 4000 to 700cm^{-1}, using KBr disk technique. At first, the pure AG was mixed with KBr and disk was made. The steel specimens were prepared as described above, and were immersed in 0.5 M H_3PO_4 containing the optimum concentration (100 ppm) of inhibitor. After 24 hours of immersion, the specimens were cleaned with distilled water and dried at room temperature. Then the thin adsorbed film formed on steel surfaces was rubbed with a small amount of KBr powder and a KBr disk was prepared using this powder. The morphology of alloys surfaces after polarization test in acidic solutions containing optimum concentration of inhibitor was examined by KYKY EM3200 scanning electron microscope.

3. Results and discussion

3.1. Potentiodynamic polarization

Figure 1 illustrates the potentiodynamic polarization curves of mild steel in 0.5 M H_3PO_4 solution in the absence and presence of various concentrations of AG. The relevant parameters are gathered in Table 1 as corrosion current density (i_{corr}), corrosion potential (E_{corr}), anodic and cathodic Tafel slopes (β_a, β_c). The corrosion current density decreased as the concentration of inhibitor increased up to 100 ppm, and then decreased at higher inhibitor concentrations. Addition of inhibitor to acid media affected both cathodic and anodic branches of the polarization curves. But the corrosion potential did not change noticeably. Therefore, AG behaved as mixed-type inhibitor.

In addition to the above parameters, Table 1 presents the values of corrosion inhibition efficiency (IE) that were calculated using the below equation:

$$IE(\%) = \frac{i_{corr} - i'_{corr}}{i_{corr}} \times 100 \qquad (2)$$

where i_{corr} and i'_{corr} are the corrosion current densities in the uninhibited and inhibited cases, respectively. The IE values reveal that the inhibition is more pronounced with increasing the inhibitor concentration. Higher concentrations above 100 ppm did not affect the IE values. The results show that AG acts as an effective inhibitor.

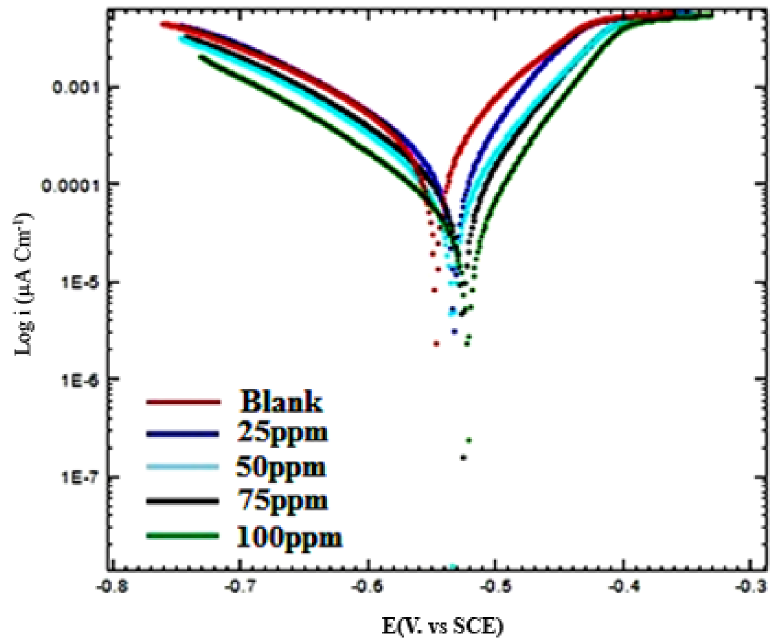

Figure 1: Polarization curves for mild steel in 0.5 M H_3PO_4 solution in the absence and presence of different concentrations of inhibitor at 25°C.

Table 1: Polarization parameters and the corresponding inhibition efficiencies for mild steel in 0.5 M H_3PO_4

C/ppm	icorr/µA cm^{-2}	Ecorr/mV	βc/mV dec^{-1}	βa/mV dec^{-1}	θ	IE(%)
blank	292.98	-548	155.17	100.45	----	----
25	191.96	-533	75.04	134.63	0.34	34
50	133.98	-534	82.18	142.93	0.54	54
75	99.64	-527	69.41	121.79	0.65	65
100	39.35	-522	106.4	55.04	0.86	86

To obtain the surface coverage, θ, it was assumed that the inhibition efficiency is due to the blocking effect of the adsorbed species and hence θ= IE(%)/100. Here, an attempt was made to test the Langmuir, Temkin, Freundluich and Frumkin isotherms. The Langmuir adsorption isotherm was found to fit well with the experimental data (Figure 2), which can be expressed as:

$$\frac{C}{\theta} = \frac{1}{K_{ads}} + C \qquad (3)$$

where θ is the surface coverage, C is the inhibitor concentration and Kads is the adsorption equilibrium constant. The plot of versus C for solutions containing inhibitor (Figure 2) yields straight line with correlation coefficient close to 1.0 (R_2 = 0.9966) confirming that the adsorption of the inhibitor is well described by the Langmuir adsorption isotherm. This isotherm is based on the assumptions that all the adsorption sites are equivalent and the ability of a molecule to be adsorbed at a given site is independent of the occupation of nearby sites [23].

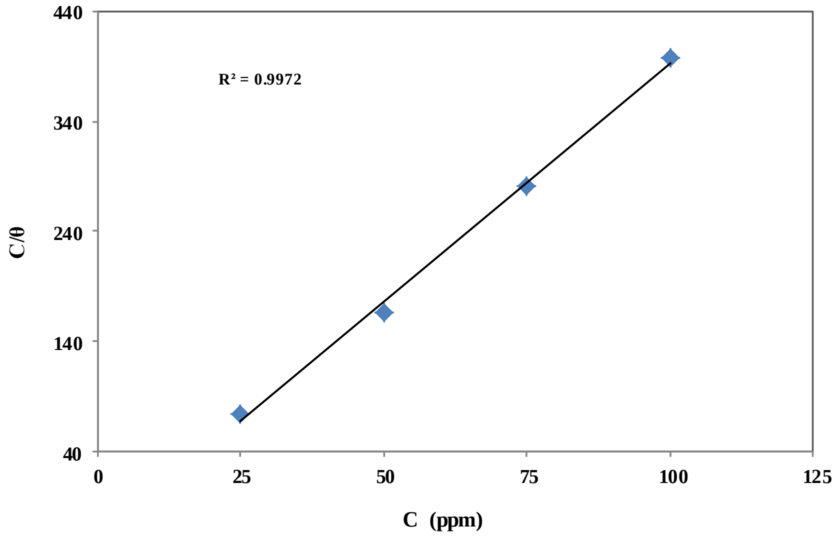

Figure 2: Langmuir adsorption isotherm of the inhibitor calculated by Tafel polarization results.

3.2. Electrochemical impedance spectroscopy

Electrochemical impedance spectroscopy (EIS) has been employed in order to investigate the surface layer created by inhibitor. The effect of apricot gum concentrations on the impedance behavior of mild steel in 0.5 M H_3PO_4 solution at 25 °C is shown in Figure 3. Inhibitor efficiency can also be estimated by charge transfer resistance according to the following equation:

$$\mathrm{IE}(\%) = \frac{R'_{ct} - R_{ct}}{R'_{ct}} \times 100 \qquad (4)$$

where R_{ct} and R'_{ct} are charge transfer resistances of mild steel in the absence and presence of inhibitor, respectively. Inhibition efficiencies increased with the concentration of inhibitor and further increase in the inhibitor concentration did not cause any appreciable change in the inhibition performance of inhibitor. Calculated efficiency by charge transfer resistance is in close correlation with those obtained from polarization results.

Figure 4 shows the electrical equivalent circuit employed to analyze the impedance plots. In this Figure, R_s is the solution resistance and R_{ct} is the charge transfer resistance. The impedance of the constant phase element (CPE) is defined as bellow [24]:

$$Z_{CPE} = A^{-1}(i\omega_{max})^{-n} \qquad (5)$$

where A is proportionality coefficient, is angular frequency (in rad. s^{-1}) and i=-1 is the imaginary number. The correct equation to convert the CPE constant, A, into the double layer capacitance, Cdl, is [25]:

$$C_{dl} = \frac{1}{2\pi f_{max} R_{ct}} \qquad (6)$$

where f_{max} is the frequency at which the imaginary component of the impedance is maximum.The electrochemical parameters, obtained from fitting the recorded EIS data are listed in Table 2. In this table are also given the calculated “double-layer capacitance” values, C_{dl}, derived from the CPE parameters and the relaxation time constant (τ) (a measure for the time required to return to the equilibrium state) according to [26]:

$$\tau = C_{dl} R_{ct} \qquad (7)$$

Inspection of the results in Table 2 indicates that the R_{ct} values increase as the concentration of inhibitor increased and the values of C_{dl} decreased with increasing the inhibitor concentration.

3.3. Linear polarization resistance

LPR method is another useful and fast method for study of inhibitors. The effect of inhibitor concentration on R_p values at 25 °C has been measured and listed in Table 2. It has been found from the LPR studies that the polarization resistance (R_p) values (Table 2) are increased from 83.20 for that of blank to 378.40 for the highest concentration of inhibitor, indicating the good inhibition character of the AG. LPR results confirm the conclusions obtained from potentiodynamic polarization and EIS results. The inhibition efficiency is calculated using the relationship:

$$IE(\%) = \frac{R'_p - R_p}{R'_p} \times 100 \qquad (8)$$

where R_p and R'_p are the polarization resistance values without and with the addition of inhibitor to the solution, respectively.

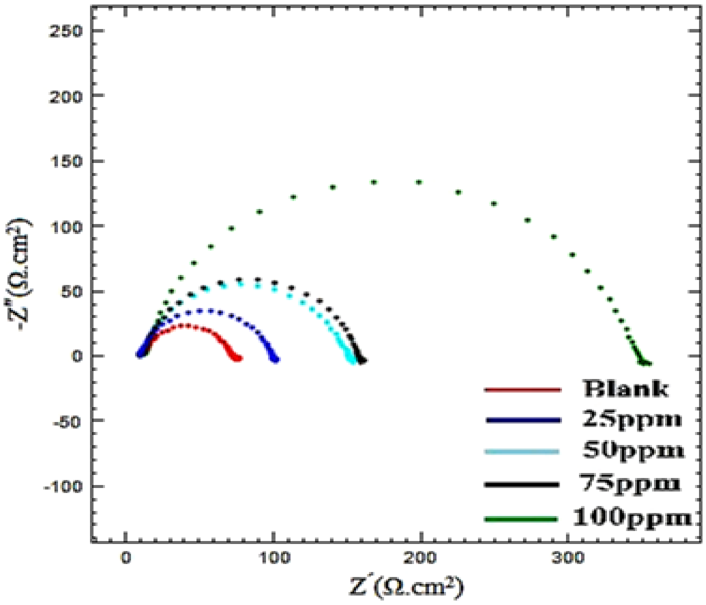

Figure 3: Nyquist plots for mild steel in 0.5 M H_3PO_4 solution in the absence and presence of different concentrations of inhibitor at 25°C.

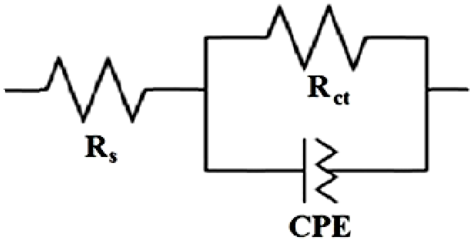

Figure 4: The electrical equivalent circuit used to fit the experimental EIS data.

Table 2: Impedance parameters data for mild steel in 0.5 M H_3PO_4 containing different concentrations of inhibitor at 25°C.

C/ppm	Rs/Ω cm^2	Rct/Ω cm^2	Cdl/μF cm^{-2}	τ/s	IE(%)
blank	8.96	64.117	34.5	0.0022	--
25	8.54	91.6	32.5	0.003	30
50	9.62	141	31.4	0.0044	54
75	10.4	150	29.8	0.0045	57
100	12.1	335	21.3	0.0071	81

Table 3: LPR results for mild steel in 0.5 M H_3PO_4 containing different concentrations of inhibitor at 25°C.

C/ppm	Rp/Ω cm^2	IE(%)
blank	83.2	--
25	106.84	22
50	173.29	51
75	178.82	53
100	378.4	78

3.4. Electrochemical noise measurements

The electrochemical noise measurements were performed on two identical working electrodes of mild steel in the 0.5 M H_3PO_4 solution. The electrochemical noise signals of current and potential obtained for mild steel in the absence and presence of various concentrations of apricot gum are shown in Figures 5 and 6. The corresponding signals after trend removal by wavelet analysis are presented in Figures 7 and 8. Some electrochemical noise signals still show the abrupt variations at the beginning of the tests which appear as large fluctuations in the trend-removed signals (Figures 7 and 8). The statistical parameters (i.e. standard deviations of current and potential) were calculated for the stable portion of each trend-removed signal [19]. The electrochemical noise resistance is calculated using equation (1) and the inhibition efficiency can also be obtained using equation (9):

$$\mathrm{IE}(\%) = \frac{R'_n - R_n}{R'_n} \times 100 \tag{9}$$

where R_n and R'_n represent the noise resistance of samples exposed to the uninhibited and inhibited solutions, respectively.

Another statistical parameter is Localization index(LI), which is calculated as:

$$\mathrm{LI} = \frac{\sigma_i}{I_{rms}} \tag{10}$$

where σ_i is the current standard deviation and I_{rms} is the current root mean square value [27]. LI has been correlated with the tendency toward localized or uniform corrosion. For LIs between 1 and 0.1, the alloy is highly susceptible to localized corrosion; for LI values between 0.01 and 0.001, the alloy is highly susceptible to uniform corrosion. Finally, for LI values between 0.1 and 0.01, the alloy is susceptible to a mixture of localized and uniform corrosion.

The electrochemical noise parameters obtained for mild steel in the 0.5 M H_3PO_4 solution in the absence and presence of various concentrations of apricot gum are gathered in Table 3.

It can be seen from the table that the inhibition efficiencies are consistent with those extracted from the four investigated electrochemical methods. Moreover, a good correlation exists between electrochemical noise resistance (R_n), linear polarization resistance (R_p) and charge transfer resistance (R_{ct}) values. LI values are obtained between 1 and 0.1, which proves that the alloy is susceptible to localized corrosion.

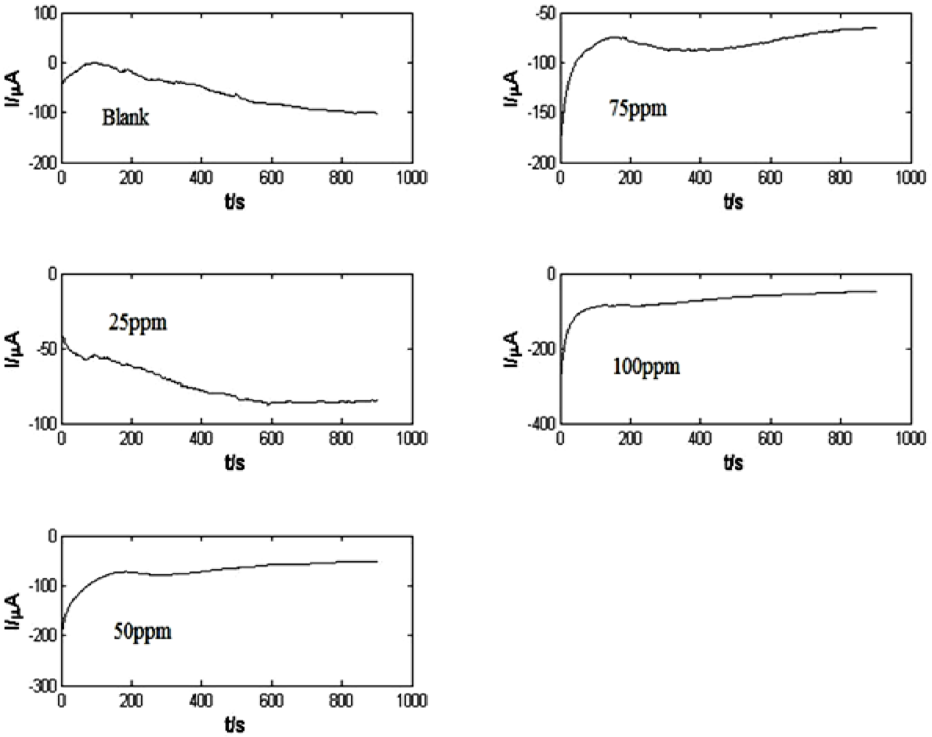

Figure 5: EN current records for mild steel in 0.5 M H_3PO_4 solution in the absence and presence of different concentrations of inhibitor at 25°C.

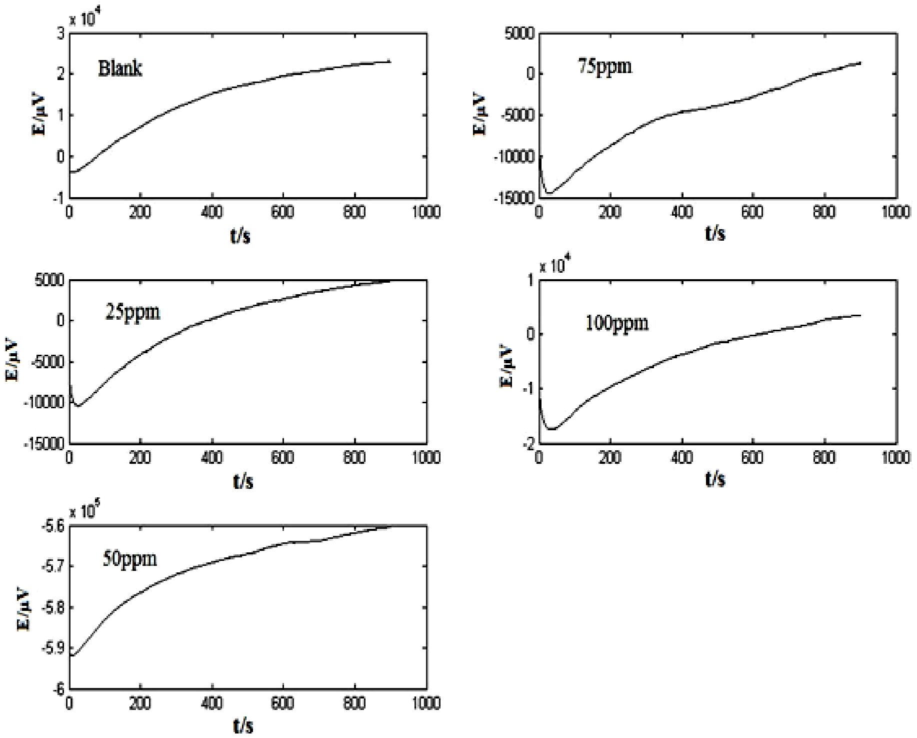

Figure 6: EN potential records for mild steel in 0.5 M H_3PO_4 solution in the absence and presence of different concentrations of inhibitor at 25°C.

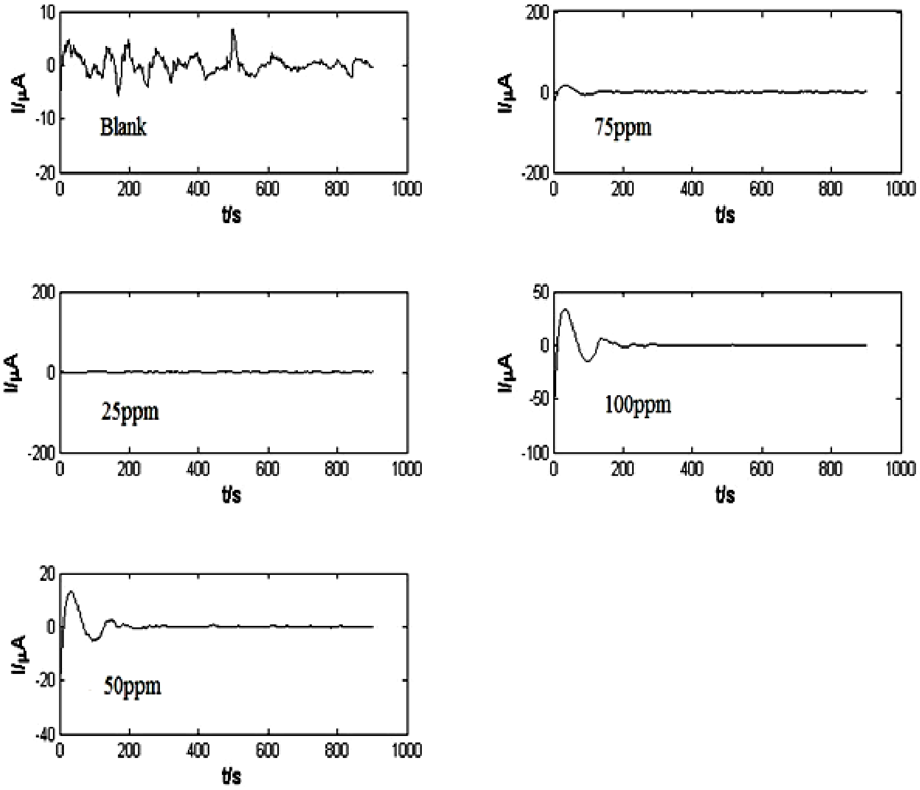

Figure 7: The trend-removed EN current records for mild steel in 0.5 M H_3PO_4 solution in the absence and presence of different concentrations of inhibitor at 25°C.

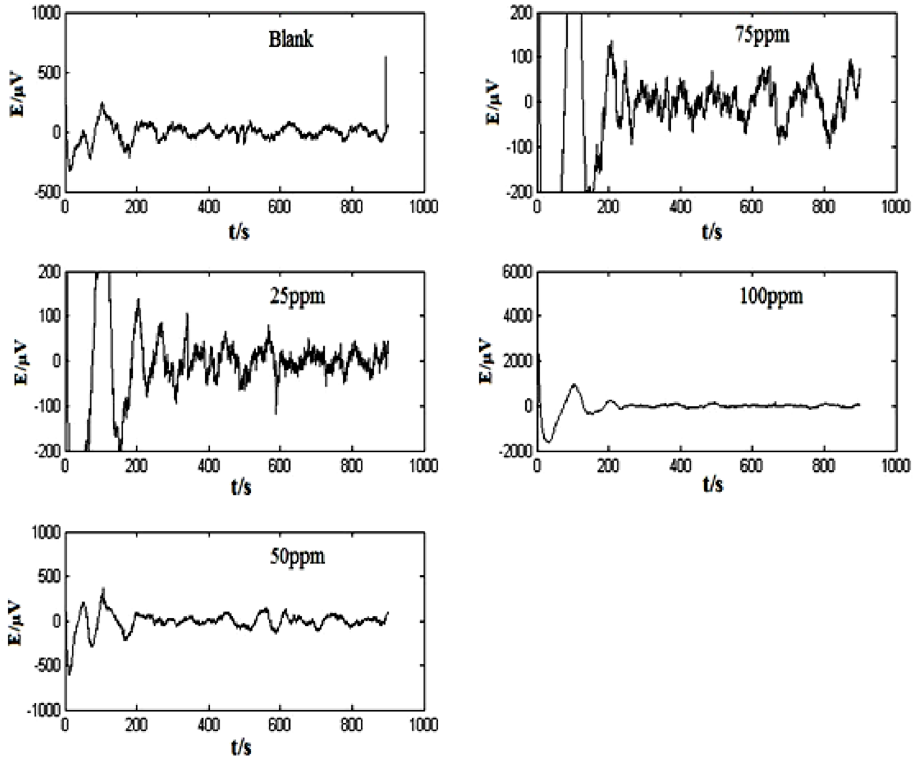

Figure 8: The trend-removed EN potential records for mild steel in 0.5 M H_3PO_4 solution in the absence and presence of different concentrations of inhibitor at 25°C.

The WT was employed to decompose each set of data points and the SDPS plots of signals in Figure 5 were obtained as shown in Figure 9. The SDPS plots can be used for calculation of the amount of noise charges at the particular frequency interval. The maximum peak in SDPS plots corresponds to predominant transients in the original EN signal [18]. However, it should be verified using the original EN signal that this maximum peak arises from the single transients rather than from the overlapped transients. Comparison between partial and original signals provides another way of recognizing the scale of the predominant transients [14]. The predominant transients can be attributed to the metastable pits. The development of a pit causes a quantity of electric charge to flow in the circuit which can be estimated by the following equation:

$$Q = i_{\max} . \tau_{\max} \qquad (11)$$

where $i_{\max}$ is the SDPS value at the maximum peak crystal ($d_{\max}$) and $\tau_{\max}$ is the average time width of $d_{\max}$ crystal. The corrosion inhibition efficiency can be defined as follows [15]:

$$IE(\%) = \frac{Q - Q'}{Q} \times 100 \qquad (12)$$

where Q and Q' are the noise charges in the uninhibited and inhibited cases, respectively.

It is evident from the SDPS plot of Blank signal (Figure 9) that the maximum is located at d4 crystal with the SDPS value of 168 nA ($i_{\max}$). The values of the parameters derived from all the SDPS plots in Figure 9 are summarized in Table 4 ($d_{\max}$, $\tau_{\max}$ and $i_{\max}$). When an SDPS plot does not exhibit an obvious maximum, it is necessary to compare the partial signals with the original signal in order to recognize the scale of the predominant transients [14]. Table 4 also presents Q and IE values. These IE values are in good agreement with those obtained from electrochemical noise resistance.

Table 4: Parameters obtained from statistical analysis of EN data for mild steel in 0.5 M H_3PO_4 containing different concentrations at 25°C.

C/ppm	σI	σV	Rn	IE(%)
blank	1.44	80.71	56.04	----
25	0.62	56.59	91.27	38
50	0.36	43.99	122.19	54
75	0.22	56.91	258.68	78
100	0.19	90.91	478.47	88

Table 5: Parameters obtained from wavelet analysis of EN data for mild steel in 0.5 M H_3PO_4 containing different concentrations of inhibitor at 25°C.

C/ppm	dmax	Δt/s	SDPS/nA	Q/Coul	IE(%)
Blank	d4	3	168	504	----
25	d4	3	116	348	31
50	d4	3	93	279	45
75	d3	1.5	43.8	65.7	87
100	d3	1.5	33	49.5	90

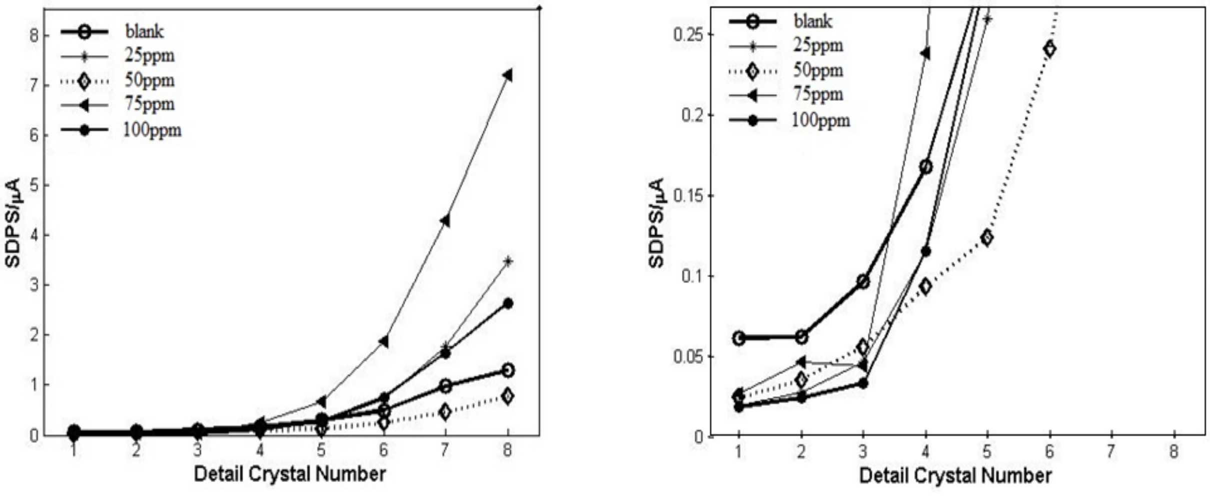

(a)

(b)

Figure 9: (a) SDPS plot of signals in Figure 5 and (b) its enlargement.

3.5. Temperature effect and thermodynamic parameters

The effect of temperature on the inhibitive performance of AG for mild steel in 0.5 M H_3PO_4 was studied by potentiodynamic polarization measurements at optimum concentration of AG. The polarization curves in the absence and presence of 100 ppm AG and in temperature range of 25–55 °C are illustrated in Figures 10 and 11, respectively. The corrosion parameters are listed in Table 5. The results obtained from polarization curves showed an increase in current density and a decrease in IE values with increasing temperature. This decrease in inhibition efficiency with increase in temperature can be explained in terms of physical adsorption of inhibitor molecule on alloy surface. In the case of physical adsorption, the extent of adsorption decreases with rise in temperature whereas the extent of desorption increases.

Some information on the mechanism of the inhibitor action can be obtained by comparing apparent activation energy (E_a), obtained in the presence of inhibitor with that in its absence. The values of E_a were calculated using Arrhenius equation:

$$i_{corr} = A\exp\left(\frac{-E_a}{RT}\right) \tag{13}$$

where i_{corr} is corrosion current, A is a constant and T is the temperature. The E_a values were determined from the Arrhenius plots [log i_{corr} versus 1/T (Figure 12)]. The calculated E_a values were 22.32 and 43.44 kJ mol^{-1} for the corrosion process in the absence and presence of AG, respectively. The increase in E_a after the addition of the AG to the 0.5 M H_3PO_4 solution indicates that physical adsorption (electrostatic) occurs in the first stage. The higher E_a value in the inhibited solution can be correlated with the increased thickness of the double layer, which enhances the activation energy of the corrosion process [28].

The standard free energy of adsorption (ΔG°_{ads}) for all the inhibitor systems are determined using the following equation [29]:

$$\Delta G^{\circ}_{ads} = -RT\ln(1\times10^{6}K_{ads}) \tag{14}$$

where 1106 is the concentration of water molecules expressed in mg L^{-1}, R is the gas constant (8.314 J $K^{-1}mol^{-1}$) and T is the absolute temperature (K). The calculated value for ΔG°_{ads} is -24.77 kJ mol^{-1}. Generally, the values of ΔG°_{ads} around 20 kJ mol^{-1} or lower are consistent with the electrostatic interaction between charged organic molecules and the charged metal surface (physisorption); those around 40 kJ mol^{-1} or higher involve charge sharing or transfer from the organic molecules to the metal surface to form a coordinate type of bond (chemisorption) [30]. In this work, the calculated ΔG°_{ads} values are in the intermediate range indicating that the adsorption of inhibitor molecules is not only physisorption or chemisorption but obeying a comprehensive adsorption (physical and chemical adsorption).

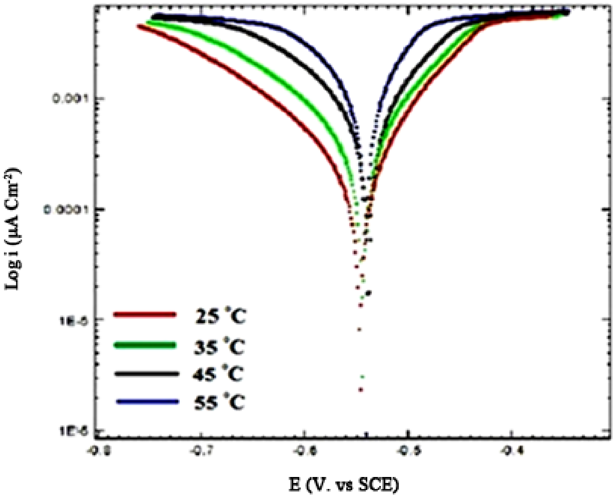

Figure 10: Effect of temperature on the polarization curves in 0.5 M H_3PO_4 solution without inhibitor.

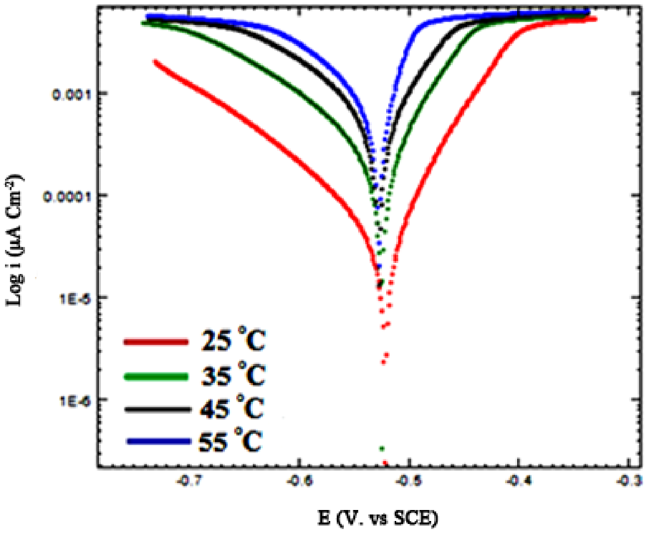

Figure 11: Effect of temperature on the polarization curves in 0.5 M H_3PO_4 solutionin the presence of 100 ppm of inhibitor.

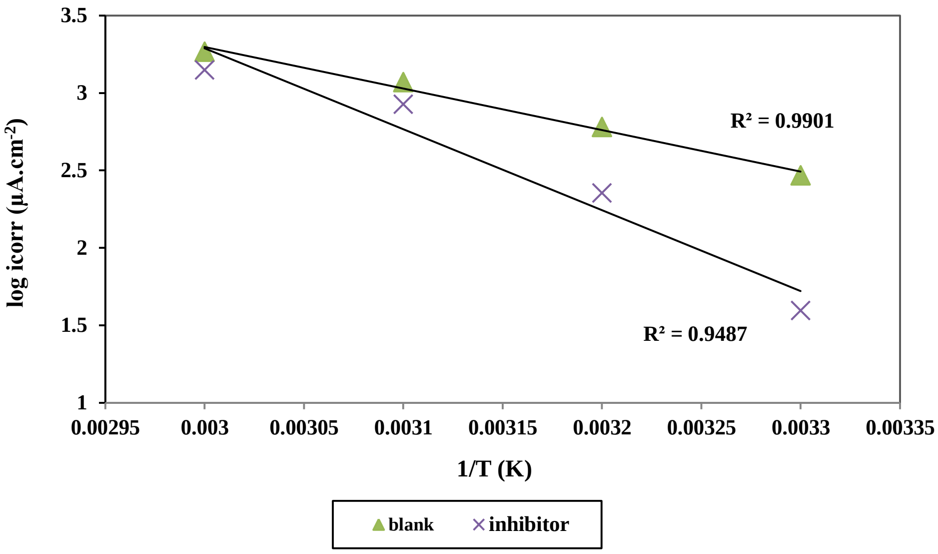

Figure 12: Arrhenius plots for mild steel in 0.5 M H_3PO_4 solution in the absence and presence of 100 ppm of inhibitor.

The Langmuir adsorption isotherm can be expressed by the following equation [31]:

$$\mathrm{Ln}\frac{\theta}{1-\theta} = \mathrm{LnA} + \mathrm{LnC} - \frac{\Delta H^{\circ}_{ads}}{RT} \qquad (15)$$

where θ is surface coverage, A is an independent constant, C is concentration, R is gas constant, T is absolute temperature and ΔH°_{ads} is enthalpy of adsorption. The plot of ln(θ/(1-θ)) versus 1/T at constant additive concentration gives a straight line as shown in Figure 13. The heat of adsorption can be obtained from the slope of the line, which is equal to $(-\Delta H^{\circ}_{ads}/R)$.

The entropy of adsorption process (ΔS°_{ads}) can also be calculated based on the following thermodynamic basic equation:

$$\Delta G^{\circ}_{ads} = \Delta H^{\circ}_{ads} - T\Delta S^{\circ}_{ads} \qquad (16)$$

ΔH°_{ads} and ΔS°_{ads} values are 30.94 kJ mol^{-1} and0.15 kJ $mol^{-1}K^{-1}$, respectively. Valuable information about the mechanism of corrosion inhibition can be provided by the values of thermodynamic parameters for the adsorption of inhibitor. An endothermic adsorption process ($\Delta H^{\circ}_{ads} > 0$) is due to chemisorption while an exothermic adsorption process ($\Delta H^{\circ}_{ads} > 0$) may be attributed to physisorption, chemisorption or a mixture of both [32]. When the process of adsorption is exothermic, physisorption can be distinguished from chemisorptions according to the absolute value of ΔH°_{ads}. For physisorption processes, this magnitude is usually lower than 40 kJ mol^{-1} while its value is around100 kJ $mol^{-1}$for chemisorptions [33]. In this work, the positive sign of ΔH°_{ads} indicates that the adsorption of inhibitors used is endothermic. Based on the results of the present work, the calculated ΔG°_{ads} and ΔH°_{ads} values for AG show that adsorption mechanismis not completely physical or chemical and a combination of physisorption and chemisorption occurs between the inhibitor and metal surface. The positive sign of ΔS°_{ads} arises from substitutional process, which can be attributed to the increase in the solvent entropy and more positive water desorption entropy [34]. It also interpreted with increase of disorders due to the more water molecules which can be desorbed from the metal surface by one inhibitor molecule [35, 36].

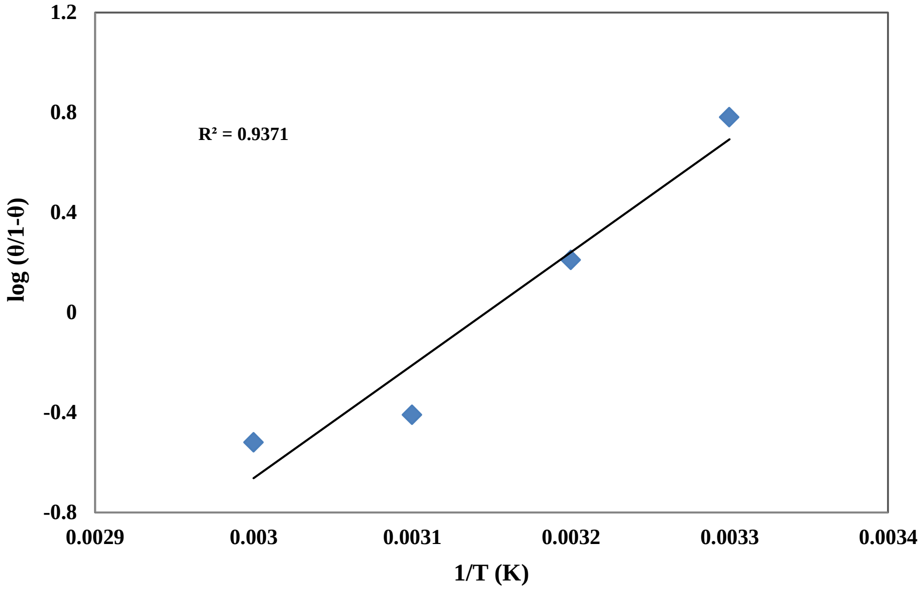

Figure 13: Plot of log (θ/1 -θ) versus 1/T for mild steel in 0.5 M H_3PO_4 solution containing 100 ppm of inhibitor at different temperatures.

3.5. SEM observations

Scanning electron micrographs (SEM) of the surface of mild steel immersed for 24 h in 0.5 M H_3PO_4 without and with the inhibitor are shown in Figure 14(a and b). Mild steel surface in phosphoric acid (Figure 14a) was drastically damaged but in the presence of 100 ppm AG (Figure 14b) surface was remarkably improved. This demonstrates the potentiality of AG to act as an efficient corrosion inhibitor for mild steel in the acidic media.

3.6. Fourier transform infrared (FT-IR) spectroscopy

Earlier researchers have confirmed that FT-IR spectrometer is a powerful instrument that can be used to determine the type of bonding for organic inhibitors adsorbed on the metal surface [37, 38]. The FT-IR spectra of pure Apricot gum and the spectra of adsorbed layer formed on carbon steel surface after 24 h immersion in 0.5 M H_3PO_4 containing 100 ppm inhibitor are shown in Figure 15 (a and b).

The FT-IR spectrum of pure compound is shown in Figure 15a. The broad peak at 3427 cm^{-1} is related to hydroxyl groups and N-H stretching. This broad peak can be related to the existence of moisture in the apricot gum. Peaks at 2926 cm^{-1}, 1616 cm^{-1} and 1035 cm^{-1} correspond to C-H stretching aliphatic, carbonyl group and C-O, respectively. The FT-IR spectra of adsorbed protective layer formed on the surface is shown in Figure 15b. As can be seen, all-important peaks in pure compound appeared in adsorption layer on the steel surface. The band around 1627 cm^{-1} is attributed to C=O stretching vibrations. Appearance of this peak in adsorbed layer indicates that oxygen atom and carbonyl group did not contribute in adsorption process. The double peaks around 2854, 2924 cm^{-1} are assigned to C-H stretching aliphatic. These peaks indicate the presence of AG in the adsorbed layer on the surface of alloy, which is approving the adsorption of inhibitor. The broad and strong peak around 3424 cm^{-1} is related to O-H stretching and indicated that the protective film is formed, containing water molecules [38].

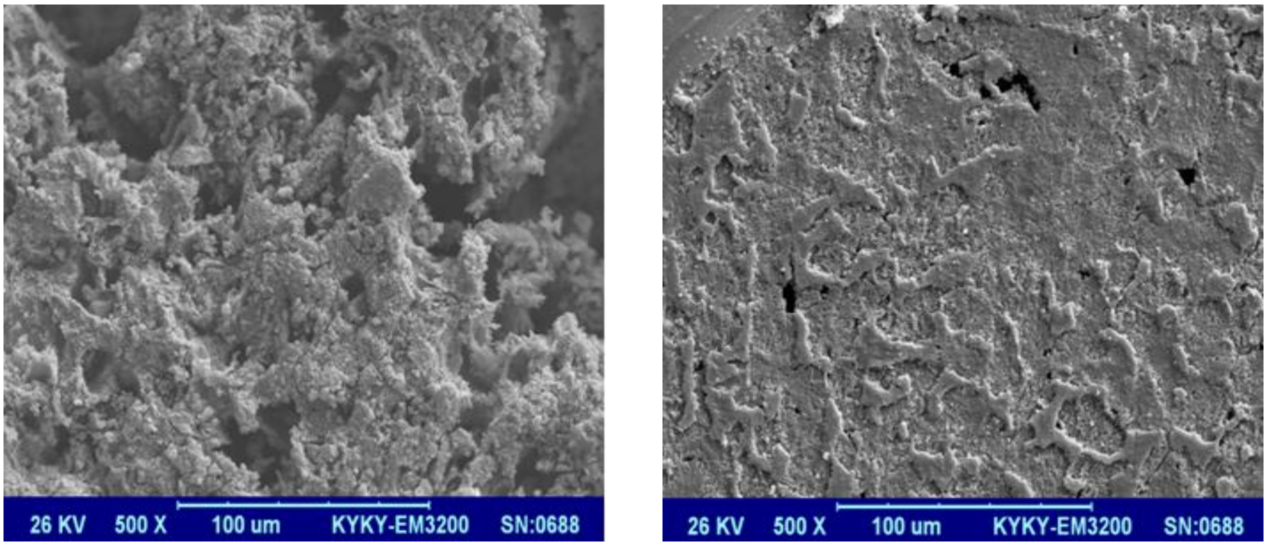

(a) (b)

Figure 14: SEM images of mild steel after immersion in 0.5 M H_3PO_4 for 24 h (a) in the absence of inhibitor (b) in the presence of 100 ppm inhibitor.

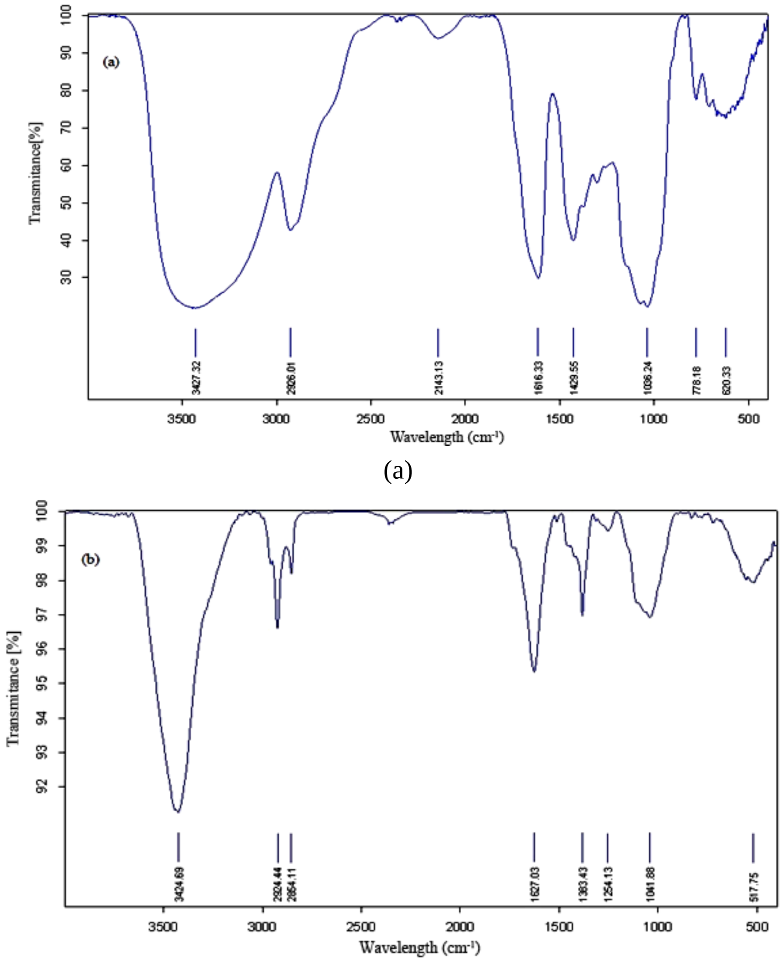

(a)

(b)

Figure 15: FT-IR of (a) pure inhibitor, (b) adsorbed layer formed on the mild steel after immersion in 0.5 M H_3PO_4 in the presence of 100 ppm inhibitor for 24 hours.

4. Conclusion

The results showed that apricot gum acts as an effective inhibitor. The inhibition efficiency increased with inhibitor concentration up to a certain concentration, and decreased with increase in temperature. Polarization curves indicated that apricot gum acts as a mixed type inhibitor. The EIS measurements showed that by addition of the inhibitor up to a certain concentration, the charge transfer resistance increases and the double layer capacitance decreases. Good agreement was observed between the results obtained from analysis of EN data and those achieved by the polarization and EIS measurements. Moreover, a good correlation was seen between electrochemical noise resistance (R_n), linear polarization resistance (R_p) and charge transfer resistance (R_{ct}) values. The adsorption studies revealed that the adsorption of the inhibitor on the alloy surface in 0.5 M H_3PO_4 followed the Langmuir isotherm. The calculated values of free energy and adsorption enthalpy indicated that both physical and chemical adsorption take place. SEM images revealed that the alloy surface damage is significantly decreased in the presence of the inhibitor.

6. References

1. M. Ozcan, R. Solmaz, G. Kardas, I. Dehri, Adsorption properties of barbiturates as green corrosion inhibitors on mild steel in phosphoric acid, *Colloid Surface A*, 325(2008), 57-63.
2. M. J. Bahrami, S. M. A. Hosseini, P. Pilvar, Experimental and theoretical investigation of organic compounds as inhibitors for mild steel corrosion in sulfuric acid medium, *Corros. Sci.*, 52(2010), 2793-2803.
3. B. D. Mert, A. O. Yüce, G. Kardas, B. Yazıcı, Inhibition effect of 2-amino-4-methylpyridine on mild steel corrosion: Experimental and theoretical investigation, *Corros. Sci.*, 85(2014), 287-295.
4. I. Ahamad, M. A. Quraishi, Bis (benzimidazol-2-yl) disulphide: An efficient water soluble inhibitor for corrosion of mild steel in acid media, *Corros. Sci.*, 51(2009), 2006-2013.
5. S. M. A. Hosseini, M. Salari, M. Ghasemi, 1-Methyl-3-pyridine-2-yl-thiourea as inhibitor for acid corrosion of stainless steel, *Mater. Corros.*, 60(2009), 963-968.
6. G. Gece, Review, Drugs: A review of promising novel corrosion inhibitors, *Corros. Sci.*, 53(2011), 3873-3898.
7. H. Tajabadipour, M. Shahidi, N. Karachi, Polarization, EIS and EN Studies to Evaluate the Inhibition Effect of Vanillin as Environment-friendly Inhibitor on Carbon Steel in Hydrochloric Acid Solution, *J. Phys. Theor. Chem. IAU Iran*, 10(Winter 2014), 231-246.
8. B. Sanyal, Organic compounds as corrosion inhibitors in different environments - *A review, Prog. Org. Coat.*, 9(1981), 165-236.
9. M. H. Hussin, M. Jain Kassim, N. N. Razali, N. H. Dahon, D. Nasshorudin, The effect of Tinospora crispa extracts as a natural mild steel corrosion inhibitor in 1 M HCl solution, Arab. J. Chem., In press (2011).
10. R. Saratha, V. G. Vasudha, Inhibition of Mild Steel Corrosion in 1N H_2SO_4 Medium by Acid Extract of Nyctanthes arbortristis Leaves, *E-J. Chem*, 6(2009), 1003-1008.
11. J. C. da Rocha, J. A. da Cunha Ponciano Gomes, E. D'Elia, Corrosion inhibition of carbon steel in hydrochloric acid solution by fruit peel aqueous extracts, *Corros. Sci.*, 52(2010), 2341-2348.
12. P. B. Raja, M. G. Sethuraman, Solanum nigrum as natural source of corrosion inhibitor for mild steel in sulphuric acid medium, *Corros. Eng. Sci. Tech.*, 45(2010), 455-460.
13. A. Lecante, F. Robert, P. A. Blandinières, C. Roos, Anti-corrosive properties of S. tinctoria and G. ouregou alkaloid extracts on low carbon steel, *Curr. Appl. Phys.*, 11(2011), 714-724.
14. M. Shahidi, A. H. Jafari, S. M. A. Hosseini, Comparison of Symmetrical and Asymmetrical Cells by Statistical and Wavelet Analysis of Electrochemical Noise Data, *Corrosion*, 68(2012), 1003-1014.
15. G. Golestani, M. Shahidi, D. Ghazanfari, Electrochemical evaluation of antibacterial drugs as environment-friendly inhibitors for corrosion of carbon steel in HCl solution, *Appl. Surf. Sci.*, 308(2014), 347-362.
16. H. Ashassi-Sorkhabi, D. Seifzadeh, M. G. Hosseini, EN, EIS and polarization studies to evaluate the inhibition effect of 3H-phenothiazin-3-one, 7-dimethylamin on mild steel corrosion in 1M HCl solution, *Corros. Sci.*, 50(2008), 3363-3370.
17. A. Aballe, M. Bethencourt, F. J. Botana, M. Marcos, Using wavelets transform in the

analysis of electrochemical noise data, Electrochim. Acta, 44 (1999) 4805-4816.

18. M. Shahidi, S. M. A. Hosseini, A. H. Jafari, Comparison between ED and SDPS plots as the results of wavelet transform for analyzing electrochemical noise data, *Electrochim. Acta,* 56(2011), 9986-9997.
19. M. J. Bahrami, M. Shahidi, S. M. A. Hosseini, Comparison of electrochemical current noise signals arising from symmetrical and asymmetrical electrodes made of Al alloys at different pH values using statistical and wavelet analysis. Part I: Neutral and acidic solutions, *Electrochim. Acta,* 148 (2014), 127-144.
20. S. Girija, U. K. Mudali, H. S. Khatak, B. Raj, The application of electrochemical noise resistance to evaluate the corrosion resistance of AISI type 304 SS in nitric acid, *Corros. Sci.,* 49(2007), 4051-4068.
21. R. A. Cottis, Interpretation of Electrochemical Noise Data, *Corrosion,* 57 (2001), 265-285.
22. A. M. Homborg, T. Tinga, X. Zhang, E. P. M. V. Westing, P. J. Oonincx, J. H. W. d. Wit, J. M. C. Mol, Time-frequency methods for trend removal in electrochemical noise data, *Electrochim. Acta,* 70(2012), 199-209.
23. P. Atkins, J. d. Paula, Physical Chemistry, W. H. Freeman and Company, New York, 2006.
24. M. Outirite, M. Lagrenée, M. Lebrini, M. Traisnel, C. Jama, H. Vezin, F. Bentiss, ac impedance, X-ray photoelectron spectroscopy and density functional theory studies of 3,5-bis(n-pyridyl)-1,2,4-oxadiazoles as efficient corrosion inhibitors for carbon steel surface in hydrochloric acid solution, *Electrochim. Acta,* 55(2010), 1670-1681.
25. M. S. Al-Otaibi, A. M. Al-Mayouf, M. Khan, A. A. Mousa, S. A. Al-Mazroa, H. Z. Alkhathlan, Corrosion inhibitory action of some plant extracts on the corrosion of mild steel in acidic media, *Arab. J. Chem.,* 7(2014), 340-346.
26. G. J. Brug, A. L. G. v. d. Eeden, M. Sluyters-Rehbach, J. H. Stuyters, The analysis of electrode impedances complicated by the presence of a constant phase element, *J. Electroanal. Chem.,* 176(1984), 275-295.
27. A. Ghauch, A. Tuqan, H. A. Assi, Antibiotic removal from water: Elimination of amoxicillin and ampicillin by microscale and nanoscale iron particles, *Environ. Pollut.,* 157(2009), 1626-1635.
28. Y. P. Khodyrev, E. S. Batyeva, E. K. Badeeva, E. V. Platova, L. Tiwari, O. G. Sinyashin, The inhibition action of ammonium salts of O,O′-dialkyldithiophosphoric acid on carbon dioxide corrosion of mild steel, *Corros. Sci.,* 53(2011) 976-983.
29. P. Roy, P. Karfa, U. Adhikari, D. Sukul, Corrosion inhibition of mild steel in acidic medium by polyacrylamide grafted Guar gum with various grafting percentage: Effect of intramolecular synergism, *Corros. Sci.,* 88(2014), 246-253.
30. G. Moretti, F. Guidi, G. Grion, Tryptamine as a green iron corrosion inhibitor in 0.5 M deaerated sulphuric acid, *Corros. Sci.,* 46(2004), 387-403.

H. Ashassi-Sorkhabi, B. Shaabani, D. Seifzadeh, Corrosion inhibition of mild steel by some schiff base compounds in hydrochloric acid, *Appl. Surf. Sci.,* 239(2005), 154-164.

32. S. F. Mertens, C. Xhoffer, B. C. D. Cooman, E. Temmerman, Short-Term Deterioration of Polymer-Coated 55% Al-Zn-Part 1: Behavior of Thin Polymer Films, *Corrosion,* 53(1997), 381-388.
33. F. Bentiss, M. Lagrenee, M. Traisnel, J.C. Hornez, The corrosion inhibition of mild steel in acidic media by a new triazole derivative, *Corros. Sci.,* 41(1999), 789-803.
34. X. Li, S. Deng, H. Fu, G. Mu, Inhibition effect of 6-benzylaminopurine on the corrosion of cold rolled steel in H_2SO_4 solution, *Corros. Sci.,* 51(2009), 620-634.
35. R. Solmaz, G. Kardas, M. Culha, B. Yazıcı, M. Erbil, Investigation of adsorption and inhibitive effect of 2-mercaptothiazoline on corrosion of mild steel in hydrochloric acid media, *Electrochim. Acta,* 53(2008), 5941-5952.
36. G. Avci, Corrosion inhibition of indole-3-acetic acid on mild steel in 0.5 M HCl, *Colloid Surface A,* 317(2008), 730-736.
37. A. Lalitha, S. Ramesh, S. Rajeswari, Surface protection of copper in acid medium by azoles and surfactants, *Electrochim. Acta,* 51(2005), 47-55.
38. Q. Qu, S. Jiang, W. Bai, L. Li, Effect of ethylenediaminetetraacetic acid disodium on the corrosion of cold rolled steel in the presence of benzotriazole in hydrochloric acid, *Electrochim. Acta,* 52(2007), 6811-6820.

How to cite this article:
A. Mohammadi, S. M. A. Hosseini, M. J. Bahrami, M. Shahidi, Corrosion Inhibition of Mild Steel in Acidic Solution by Apricot Gum as a Green Inhibitor, Prog. Color Colorants Coat., 9 (2016) 117-134.